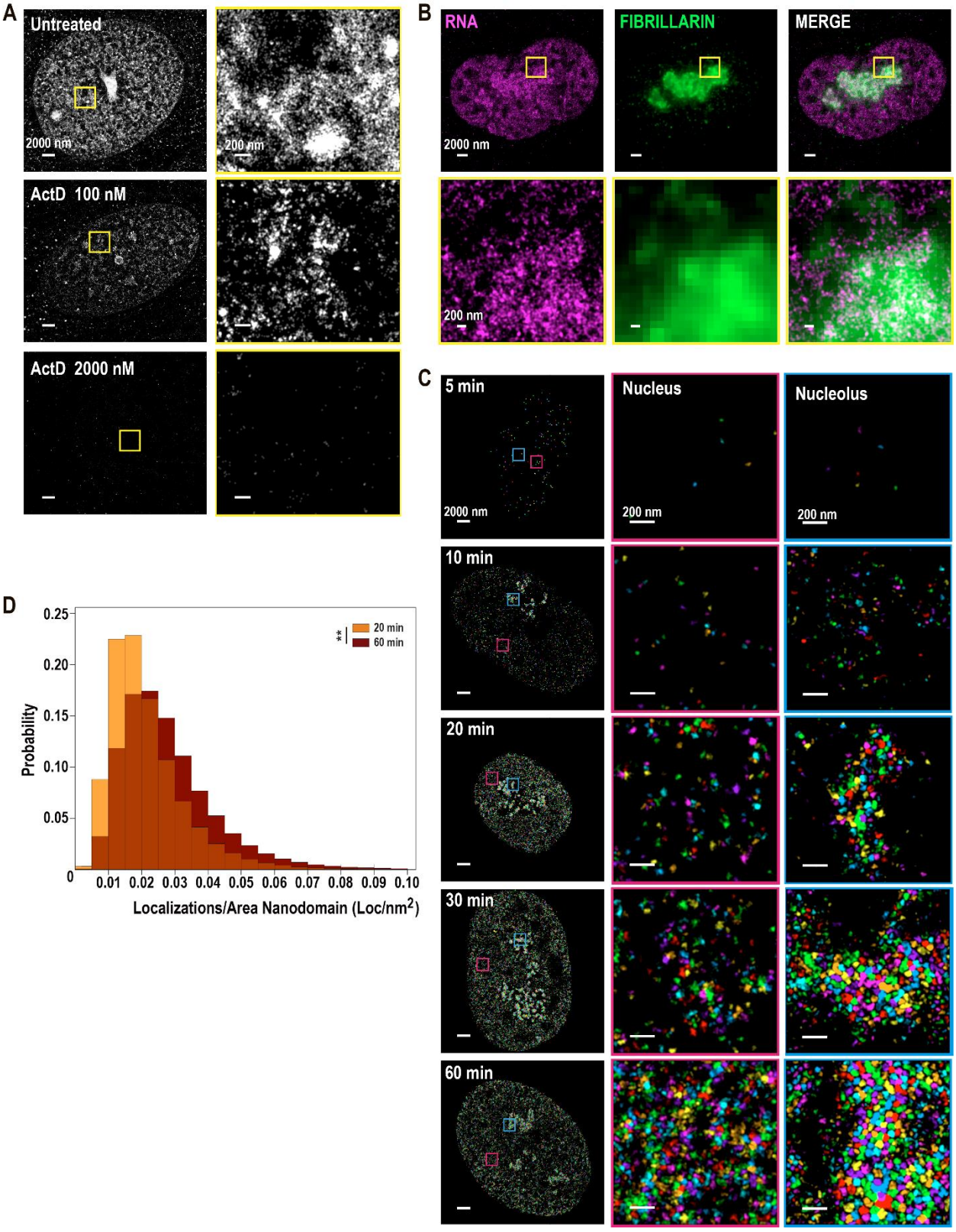
A
Untreated
2000 nm
200 nm
ActD 100 nM
ActD 2000 nM
B
RNA
FIBRILLARIN
MERGE
2000 nm
200 nm
C
5 min
10 min
20 min
30 min
60 min
Nucleus
Nucleolus
2000 nm
200 nm
D
20 min
60 min
**
Probability
0.25
0.20
0.15
0.10
0.05
0
0.01 0.02 0.03 0.04 0.05 0.06 0.07 0.08 0.09 0.10
Localizations/Area Nanodomain (Loc/nm2)

Supplementary Figure S1. EU labelling specifically labels nascent RNAs. Cluster analysis can be used to identify RNA nanodomains.

A. Representative STORM renderings of nuclear nascent RNA distribution after Actinomycin D (ActD) treatment. Human BJ fibroblasts (hFibs) shown using the conventional rendering in which localizations are represented as Gaussians with a fixed width (9 nm). Images quantitatively show the differences in RNA density following RNA polymerase (RNAP) I inhibition (100 nM ActD treatment) and RNAP I and II inhibition (2000 nM ActD treatment). Left panels show full nuclei while right panels show the zoomed nuclear areas in the yellow squares.

B. Representative STORM renderings of nascent RNA (left), conventional imaging of Fibrillarin (middle) and its merge (right). Images show the overlap between nucleolar Fibrillarin and high-density RNA signal.

C. Representative STORM images of nascent RNA data after cluster analysis. Each cluster is arbitrarily colored in order to facilitate visual identification. (Left) Full nucleus. (Middle) Zoom of nucleoplasmic region inside the magenta square. (Right) Zoom of the nucleolar region inside the cyan square.

D. Probability histogram distribution of cluster density, measured as the ratio between localizations and area of each cluster for 20 min (N=22) and 60 min (N=11). Asterisks indicate statistical significance of the separation between the mean of the medians according to unpaired two-tailed t-test. ns $p>0.05$; * $p<0.05$; ** $p<0.01$; *** $p<0.001$; **** $p<0.0001$.

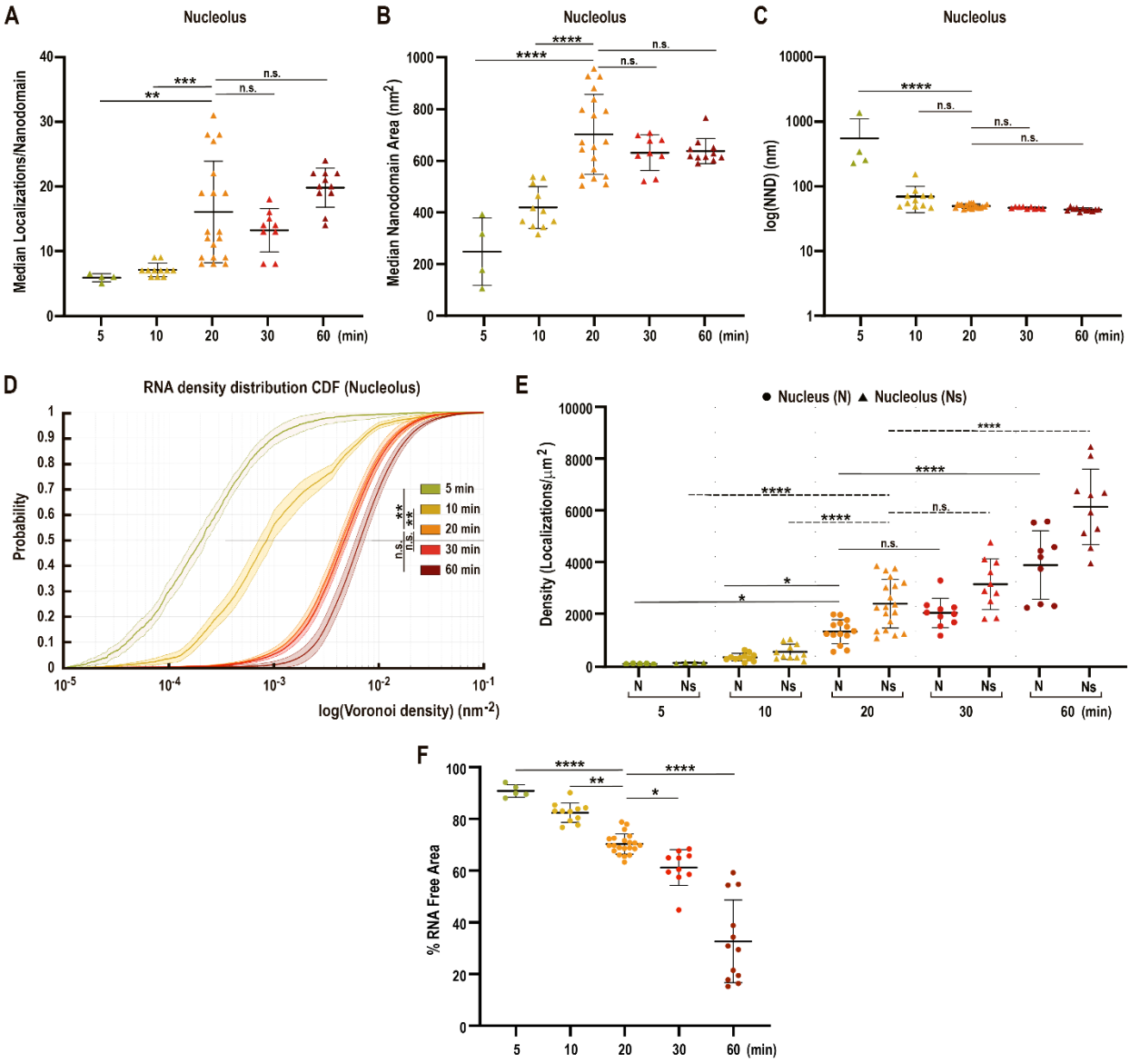

Supplementary Figure S2. Nucleolar RNA distribution follows a comparable trend as the nucleus.

A-C. Dot plots showing the median number of localizations per nanodomain (A), median area per RNA nanodomain (B) and nearest neighbor distance (NND) between RNA nanodomains (C) in nucleoli for 5 (N=5), 10 (N=11), 20 (N=22), 30 (N=10) and 60 min (N=11 cells) EU pulses in hFibs. Asterisks indicate statistical significance of the separation between the mean of the medians according to One-way ANOVA followed by Tukey's multiple comparison test against 20 min. ns $p>0.05$; * $p<0.05$; ** $p<0.01$; *** $p<0.001$; **** $p<0.0001$.

D. Cumulative distribution of the Voronoi Polygon densities for 5 (N=5), 10 (N=11), 20 (N=22), 30 (N=10) and 60 min (N=11) pulses of nascent nucleolar RNA labelling. 20 and 30 min are mostly overlapping. The light colors show the interquartile range (25–75 percentiles) and the thick lines show the median values; asterisks indicate statistical significance of the separation between the mean of the medians according to Kruskal-Wallis followed by Dunn's multiple comparison test comparing against 20 min. ns $p>0.05$; * $p<0.05$; ** $p<0.01$; *** $p<0.001$; **** $p<0.0001$.

E. Dot plots showing localization density in the nucleoplasm excluding nucleolus (circles) and in the nucleolus (triangles) for 5 (N=5), 10 (N=11), 20 (N=22), 30 (N=10) and 60 min (N=11) pulses of nascent nuclear RNA labelling in hFibs. Asterisks indicate statistical significance of the separation between the mean of the density according to One-way ANOVA followed by Dunnet's multiple comparison test against 20 min. ns $p>0.05$; * $p<0.05$; ** $p<0.01$; *** $p<0.001$; **** $p<0.0001$.

F. Dot plots showing percentage of RNA free area in the nucleus for 5 (N=5), 10 (N=11), 20 (N=22), 30 (N=10) and 60 min (N=11) pulses of nascent RNA labelling in hFibs. Asterisks indicate statistical significance of the separation between the mean of the density according to One-way ANOVA followed by Dunnet's multiple comparison test against 20 min condition. ns $p>0.05$; * $p<0.05$; ** $p<0.01$; *** $p<0.001$; **** $p<0.0001$.

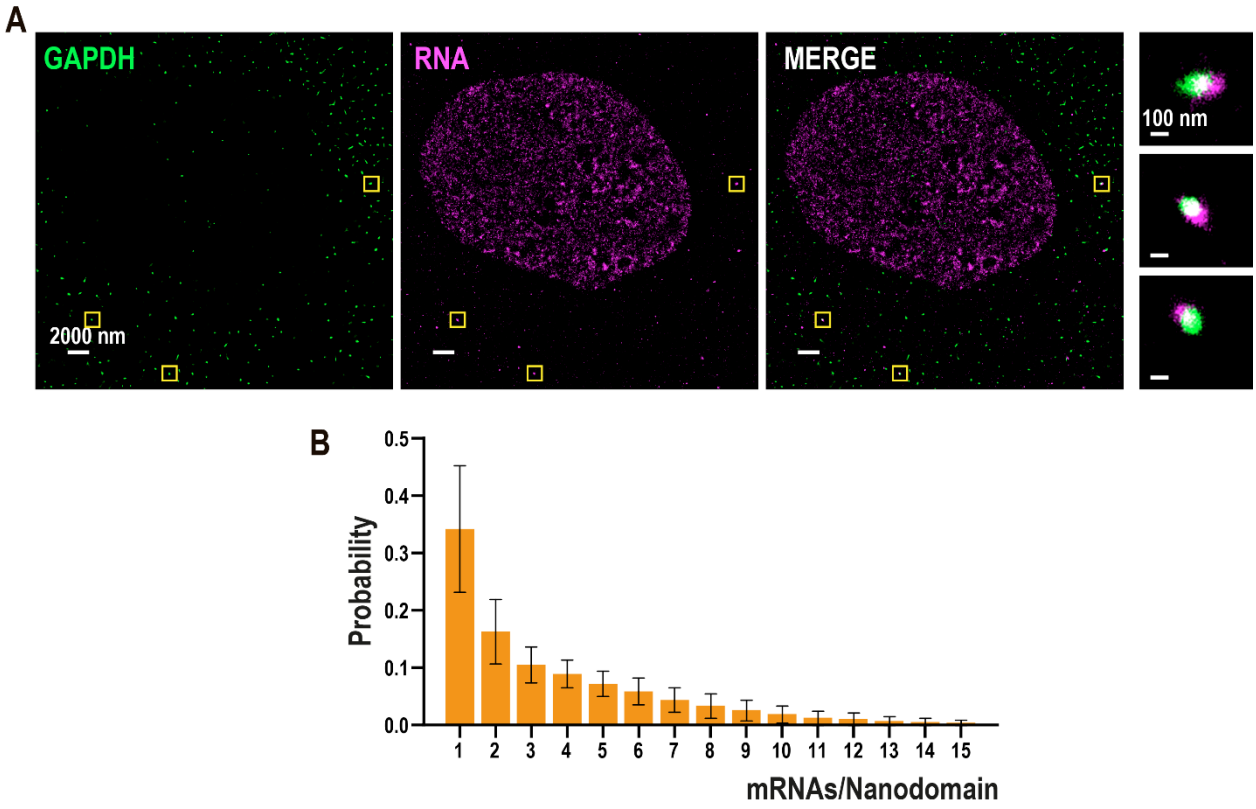

Supplementary Figure S3. Nanodomains are mostly comprised of few RNAs.

A. Representative simultaneous STORM imaging of nascent transcriptome and Stellaris smRNA-FISH for *GAPDH* in hFibs. Nascent RNA (in purple) and *GAPDH* smRNA-FISH signal (in green) are shown. (Right) Zooms of the regions in the yellow boxes show examples of overlap between cytoplasmic RNA and *GAPDH* smFISH signal.

B. Probability histogram of the distribution of RNA molecules per nucleoplasmic nanodomain.

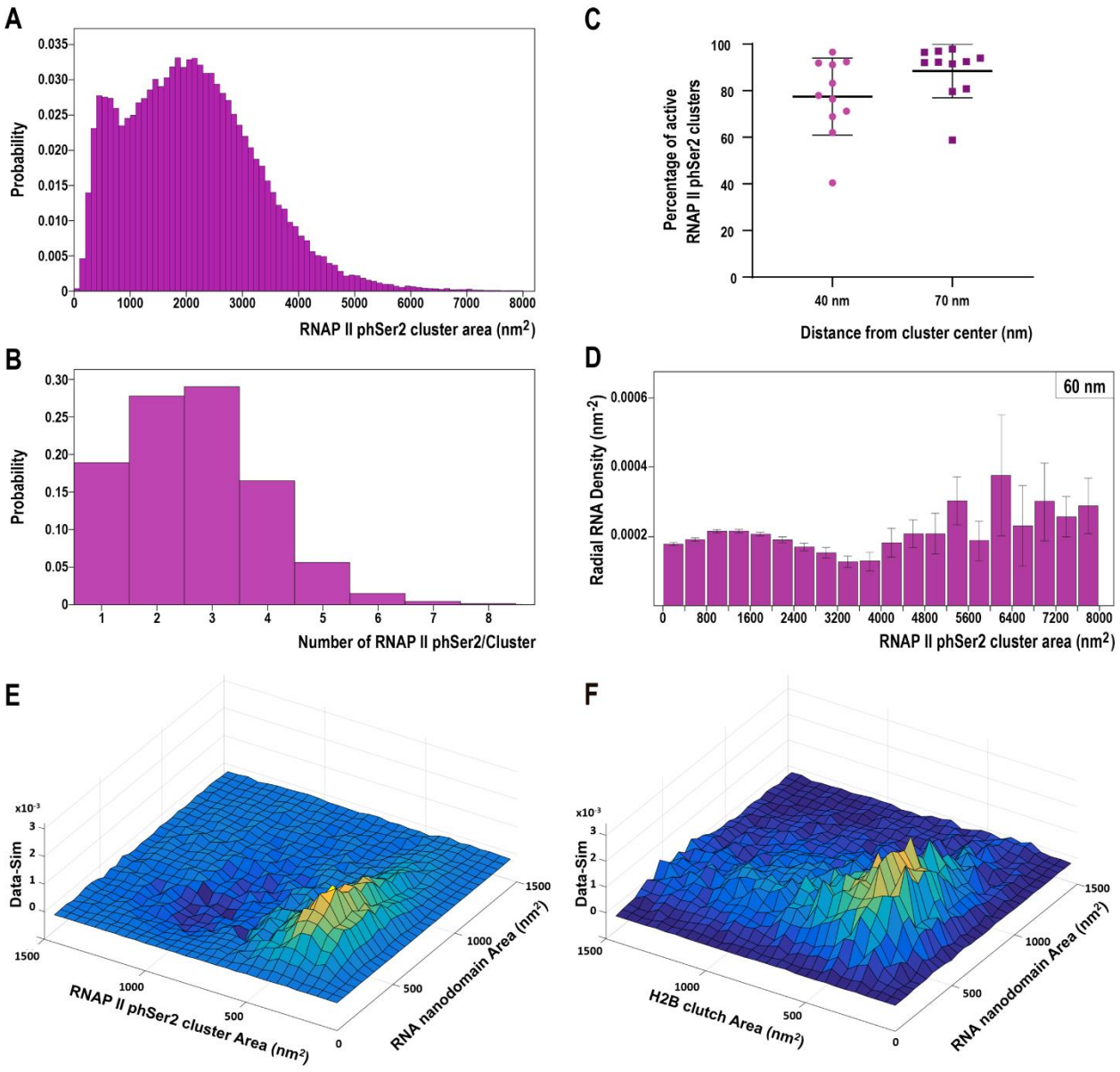

Supplementary Figure S4. Distribution of RNAP II phSer2 cluster size and its relation with RNA radial density.

A. Probability histogram distribution of RNAP II phSer2 cluster area inside the nucleus (N=6). The first peak (at ~600 nm^2) is assumed to include clusters formed by one single RNAP II phSer2 molecule. The second peak (at ~2000 nm^2) is composed of bigger clusters with more than one RNAP II phSer2 molecule.

B. Probability histogram distribution of RNAP II phSer2 molecules per cluster, normalized on the size of the first peak in Supplementary Figure S4A.

C. Percentage of active RNAP II phSer2 clusters measured as percentage of overall clusters (N= 11 cells) that have at least one localization of RNA at a distance of 40 nm from the cluster centroid.

D. RNA density in a bound ring of 60 nm versus RNAP II cluster size measured as area of the cluster in nm^2. Area is calculated taking the σ of the cluster size as radius. Columns correspond to the median RNA density at that particular cluster size, the bar corresponds to the standard deviation.

E. Enrichment of small clusters of RNAP II phSer2 associated to RNA nanodomains. Surface plot showing the difference in the association of RNA nanodomains and RNAP II phSer2 clusters over association-independent of size simulated data. N=11.

F. Enrichment of small H2B clutches associated to RNA nanodomains. Surface plot showing the difference in the association of RNA nanodomains and H2B clutches over association-independent of size simulated data. N=6.

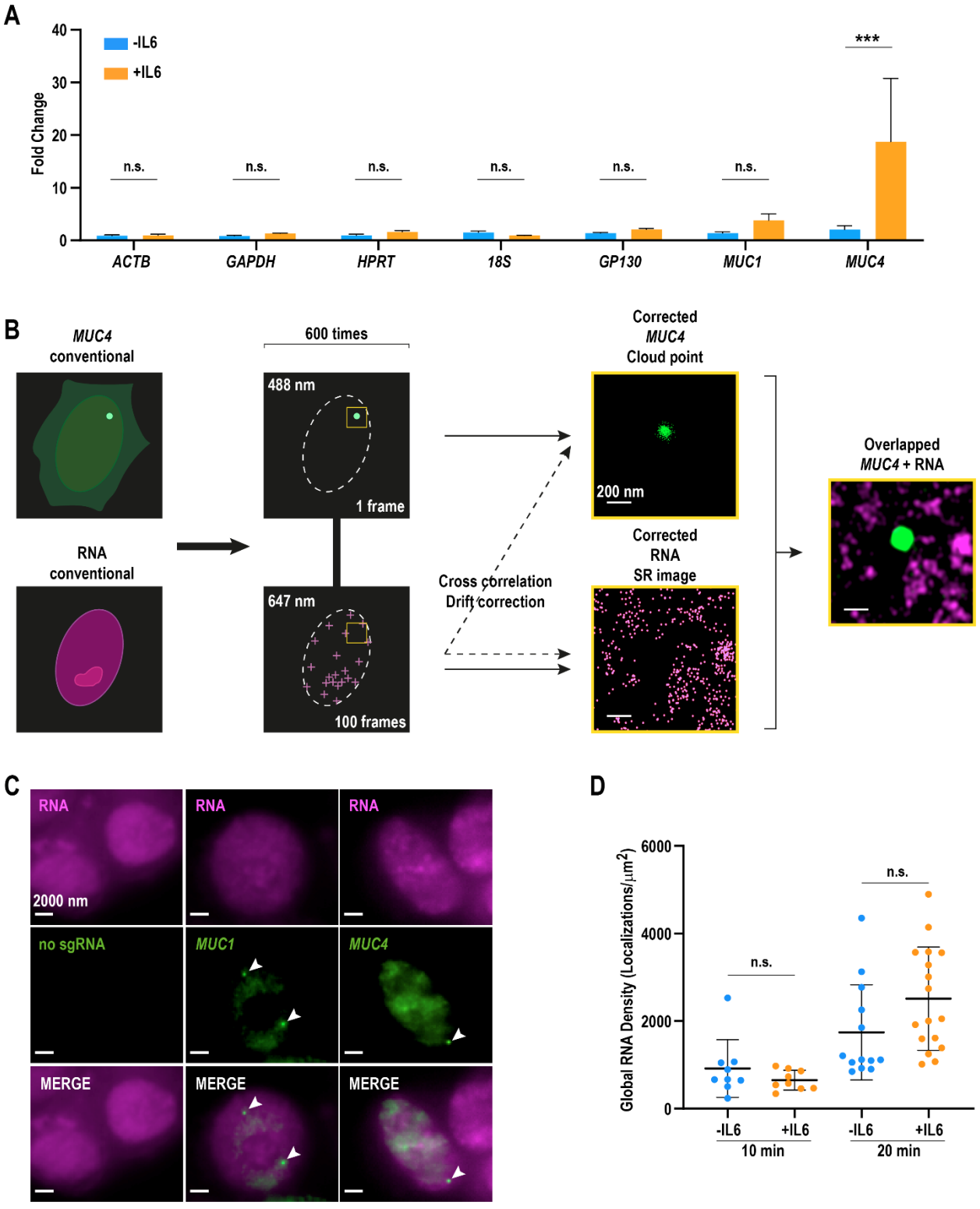
A
-IL6
+IL6
Fold Change
40
30
20
10
0
n.s.
n.s.
n.s.
n.s.
n.s.
n.s.
***
ACTB
GAPDH
HPRT
18S
GP130
MUC1
MUC4
B
MUC4
conventional
RNA
conventional
600 times
488 nm
1 frame
647 nm
100 frames
Cross correlation
Drift correction
Corrected
MUC4
Cloud point
200 nm
Corrected
RNA
SR image
Overlapped
MUC4 + RNA
C
RNA
2000 nm
no sgRNA
MUC1
MUC4
MERGE
D
Global RNA Density (Localizations/μm²)
6000
4000
2000
0
n.s.
n.s.
-IL6
+IL6
-IL6
+IL6
10 min
20 min

Supplementary Figure S5. Visualization of the transcriptionally active *MUC4* locus by FISH imaging.

A. qPCR for gene expression in -IL6 and +IL6 treated GP220 cells. ddCt expression relative to 18S and normalized to -IL6 controls. Mean and SEM values are shown for n= 4 independent experiments. Asterisks indicate statistical significance according to a One-way Anova followed by Fisher LSD test. ns $p>0.05$; *** $p<0.001$.

B. Schematic representation depicting the strategy for simultaneous imaging of the *MUC4* locus and nascent RNA. We obtain positional information of the *MUC4* locus every 100 frames of STORM to determine the centroid of the *MUC4* labelled region and to correlate it with STORM nascent RNA signal.

C. Representative GP220 cell images showing the nascent RNA conventional signal (top), no sgRNA, *MUC1* and *MUC4* STAC labelling (middle) and its merge (bottom). GFP signal is not detectable in the no sgRNA negative control. White arrows indicate *MUC1/MUC4* loci.

D. IL6 treatment does not produce a global change in amount of nascent RNA. Quantification of global RNA density in untreated and IL6 treated cells, after 10 and 20 min pulses of EU. Unpaired two tailed t-student test was performed. n.s. indicates $p>0.05$ when comparing -IL6 and +IL6 cells. (10 min N=9 for each condition, 20 min N=14 for -IL6, N=17 for +IL6).

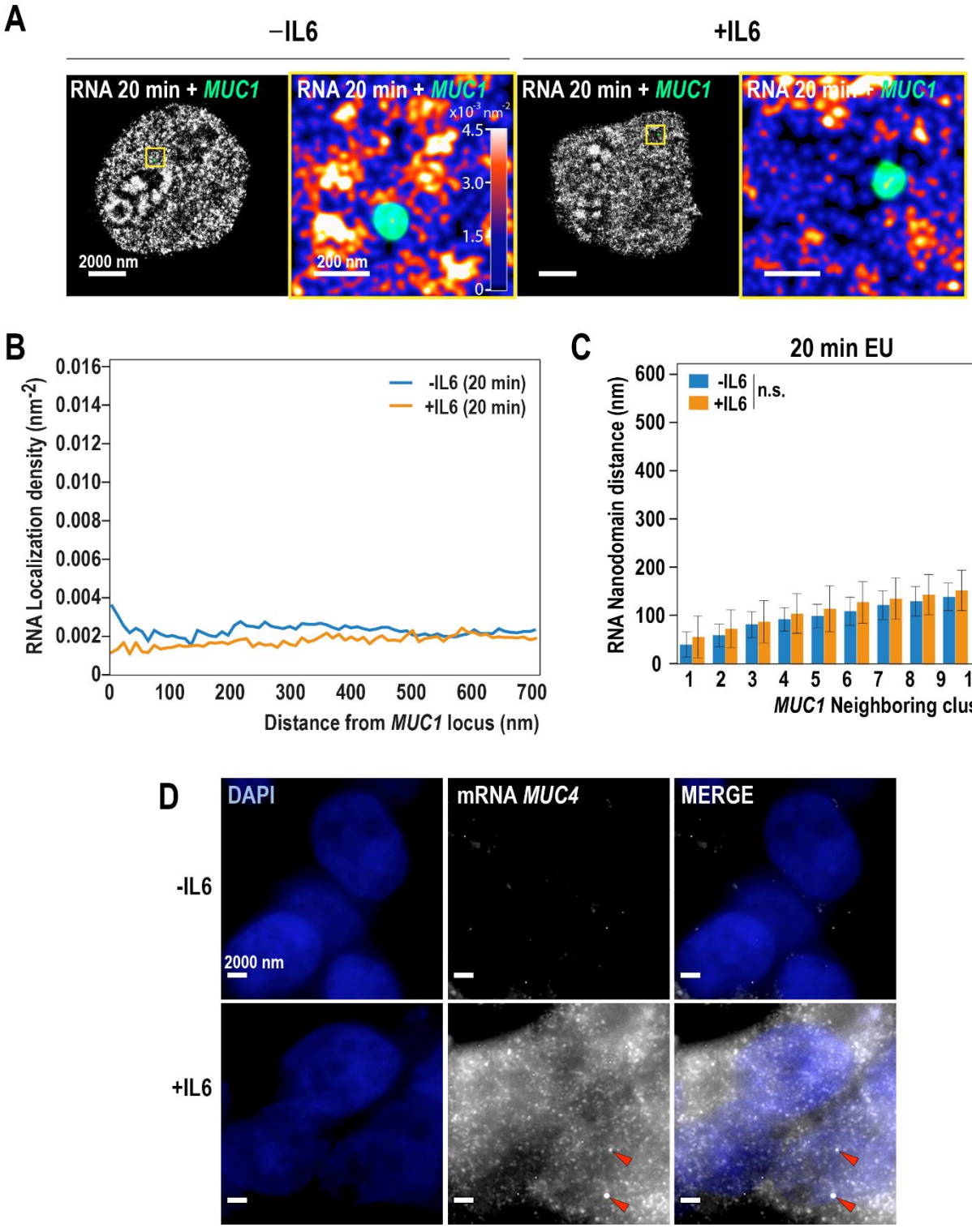
A
−IL6
+IL6
RNA 20 min + MUC1
RNA 20 min + MUC1
RNA 20 min + MUC1
RNA 20 min + MUC1
x10-3 nm-2
4.5
3.0
1.5
0
2000 nm
200 nm
B
RNA Localization density (nm-2)
0.016
0.014
0.012
0.010
0.008
0.006
0.004
0.002
0
-IL6 (20 min)
+IL6 (20 min)
0
100
200
300
400
500
600
700
Distance from MUC1 locus (nm)
C
20 min EU
RNA Nanodomain distance (nm)
600
500
400
300
200
100
0
-IL6
+IL6
n.s.
1
2
3
4
5
6
7
8
9
10
MUC1 Neighboring cluster
D
DAPI
mRNA MUC4
MERGE
-IL6
+IL6
2000 nm

Supplementary Figure S6. IL6-mediated activation of *MUC4* transcription is specific.

A. STAC labelling of *MUC1* gene locus in GP220 cells previously labelled with a 20 min pulse of EU and treated with IL6. Representative SR images of the cropped nucleus for each condition are displayed. Yellow boxes show zoomed *MUC1* loci regions (*MUC1* represented as a green point) and RNA color coded according to density.

B. Quantification of RNA density around the *MUC1* locus. Measurement of the RNA density as a function of the distance to the *MUC1* locus centroid, for cells treated with IL6 and a 20 min pulse of EU (N=8 for -IL6, N=6 for +IL6).

C. Measurement of distances between the *MUC1* locus and the nearest RNA nanodomain neighbor for 20 min EU pulses. The columns represent mean distances and the error bars show the SD between each *MUC1* locus for that particular neighbor rank (N=8 and 6 for -IL6 and +IL6, respectively). Asterisks indicate statistical significance according to a Two-way ANOVA test. ns $p>0.05$; * $p<0.05$; ** $p<0.01$; *** $p<0.001$; **** $p<0.0001$.

D. Conventional imaging of Stellaris RNA-FISH probes for *MUC4* after IL6 treatment in GP220 cells. DAPI (in blue) and *MUC4* RNA-FISH signal (in white) IL6- and IL6+ cells are shown. Red arrowheads indicate transcriptionally active loci.